Supporting Information

Johnson et al. 10.1073/pnas.1206724109

SI Materials and Methods

Antibody Generation. As immunogens, we used unique peptides from the C termini of trace amine-associated receptor (TAAR) 4 (GenPept accession no. NP_001008499, amino acids 334–347), TAAR5 (GenPept accession no. NP_001009574, amino acids 321–337), and TAAR6 (GenPept accession no. NP_778237, amino acids 332–346). The peptides were synthesized by GenScript.

RNA FISH with Immunohistochemistry. Fluorescence RNA in situ hybridization combined with immunohistochemistry experiments were performed as previously described (1). We used sense and antisense RNA probes specific for *Taar4*, *Taar5*, and *Taar6* transcripts that were labeled with digoxigenin. The sequences of these probes correspond to nucleotides 1–226 of *Taar4* (GenBank accession no NM_001008499), nucleotides 816–1014 of *Taar5* (GenBank accession no. NM_001009574), and nucleotides 739 988 of *Taar6* (GenBank accession no. NM_001010828). The probes were detected with sheep anti-digoxigenin-peroxidase. (Roche Applied Science) followed by Cy3 tyramide (PerkinElmer).

Immunohistochemistry. Except where indicated, fresh frozen tissue from adult C57/Bl6 mice were sectioned into 14-μm sections and fixed with 4% (wt/vol) paraformaldehyde in PBS for 10 min. Slides where then washed 3 × 10 min with PBS, permeabilized and quenched for 30 min in PBS + 0.1% (vol/vol) Triton X-100 (PT) + 0.3% (vol/vol) H2O2, blocked for 30 min with PT + 5% (vol/vol) donkey serum (PTS), and incubated with 1° antibodies overnight at 4 °C. Antibodies against TAAR4 and TAAR5 were used at a 1:5,000 dilution and the antibody against TAAR6 at a 1:2,000 dilution in PTS. The antibody against TAAR4 was precleared by incubation overnight at 4 °C with fixed HEK239T cells. Secondary antibodies used were either donkey anti-guinea pig Alexa Fluor 488 (Molecular Probes) or donkey anti-guinea pig HRP (Jackson ImmunoResearch) followed by Cy3 tyramide (PerkinElmer). The rabbit anti-TAAR5 antibody was detected with a goat anti-rabbit HRP secondary antibody (Santa Cruz Biotechnology) followed by Alexa Fluor 488 tyramide (Molecular Probes). All secondary antibodies were used 1:1,000 in PTS for 2 h at room temperature. For detection of β-gal, olfactory cell adhesion molecule (OCAM), and vesicular glutamate transporter 2 (VGLUT2), animals were anesthetized and transcardially perfused with 1% (wt/vol) paraformaldehyde in PBS. Primary antibodies used were chicken anti-β-gal (ab9361; Abcam) at 1:1,000, goat anti-OCAM (AF774; R&D Systems) at 1:100, and mouse anti-VGLUT2 (ab79157; Abcam) at 1:1,000. Secondary antibodies used were donkey anti-chicken Dylight 549, donkey anti-goat Dylight 488, and donkey anti-mouse Dylight 649, all at 1:500 (Jackson ImmunoResearch). Sections were counterstained with either with DAPI or TOTO-3 iodide (Molecular Probes). Images were taken using a Zeiss LSM 510 DuoScan confocal microscope and were formatted using ImageJ software.

Glomerular Distribution Maps. 14 μm sections were collected from the entire OB of adult C57/Bl6 mice and stained with antibodies against M71, TAAR4, TAAR5, or TAAR6. The position of the center of each glomerulus was defined as the distance from the anterior tip of the OB (for the *y* axis) and the distance from the midline (for the *x* axis). The OB boundary shown in each plot is for the individual animal. The position of the center of each glomerulus was defined as a percentage of the distance from the anterior tip of the OB to the anterior tip of the AOB (for the *y* axis) and the percentage of the distance from the midline to the lateral edge of the OB (for the X-axis). The boundary of the OB shown in each plot is averaged across all of the mice represented in the plot. 2D histograms of the data were used to generate the smoothed density. Mice were 4–6 wk old. TAAR4: $n = 9$; TAAR5: $n = 7$; TAAR6: $n = 7$; M71: $n = 8$.

Genotyping *Taar5*^{LacZ} Mice. Mice were genotyped by PCR using primers that recognize the WT *Taar5* allele 1N: GAAGAGCCTTGTGTGATAGAC; and 2C: CAGAGATGGAAGATGGAGGTGAG; and the LacZ knockin allele 1N and 3C: GTCTGTCCTAGCTTCCTCACTG.

Two-Color RNA FISH. The cRNA riboprobes used matched the full coding regions of *Taar*, *Olfr139*, and *Olfr142* genes (2), and partial coding regions of *Olfr77*, *Olfr821*, and *Olfr1019* genes (3). Two riboprobes matching partial LacZ sequences (1: bp 1–1500; and 2: bp 1501–3000) were combined for enhanced sensitivity. Epifluorescent images were taken using a Leica TCS SP5 II microscope. Brightness and contrast were adjusted to permit adequate visualization of images after printing.

Whole-Mount X-Gal Staining. Freshly dissected tissue was incubated (30 min, room temperature) with fixative (1% (vol/vol) formaldehyde, 0.2% (vol/vol) gluteraldehyde, 2 mM MgCl2, 5 mM EGTA, 0.02% (vol/vol) Nonidet P-40, and PBS) and washed (PBS containing 0.02% (vol/vol) Nonidet P-40, 3 × 5 min). Tissue was incubated (2–4 h, 37 °C, dark) in staining solution [1 mg/mL X-gal, 5 mM K3Fe(CN)6, 5 mM K4Fe (CN)6, 2 mM MgCl2, 0.01% (wt/vol) sodium deoxycholate, and 0.01% (vol/vol) Nonidet P-40], washed (PBS, 3 × 10 min, room temperature), post-fixed [4% (wt/vol) paraformaldehyde, PBS, 4 to 5 h, 4 °C], and stored (80% glycerol, PBS, 4 °C).

Epigenetic Analysis. The antibodies used were specific for H3 trimethyl lysine-9 (ab8898), H4 trimethyl lysine-20 (ab9051), H3 dimethyl lysine-9 (ab1220) from Abcam, and H3 trimethyl lysine-27 (07-449) from Upstate Chemicals. ChIP-on-chip experiments and data analysis were performed as previously reported (4). Quality control of the ChIP-on-chip data were performed both by NimbleGen (according to their protocols) and by our group. The log2 (ChIP/input) ratio was normalized in a "weighted global" manner. For peak analysis we used the model-based analysis of 2-color arrays (MA2C) (5), which is a variation of the general sliding window approach. We also confirmed our results by a different algorithm (6). For peak analysis, two different pipelines of existing tools were used: one was for large-organized chromatin K9 modifications (LOCKs) (6), and the other one was the MA2C (5). Both pipelines are variations on the general sliding window approach, but we adjusted the parameters to, especially, search for large-scale enrichment. In the LOCKs method, averaging was performed across 500-bp windows, whereas the minimum block size was 10,000. In the MA2C pipeline, we used the default parameters for peak finding (window of 500 bp, minimum number of probes in a window 5, and maximum gap of 250 bp) and also the adjusted parameters for large domains (window of 10 kb, minimum number of probes 20, maximum gap of 1 kb). A false discovery rate ≤5% was used in both cases.

Generation of Degenerate Odorant Receptor (OR) Probe for in Situ Hybridization. Degenerate primers were used to amplify OR sequence segments from TM3–TM6 as previously described (7).

The sequences of the degenerate primers were as follows except that a 25-bp T7 promoter sequence was added to the P27 primer:

P26:_GCITA(C/T)GA(C/T)CGITA(C/T)GTIGCIATITG
P27_T7:_AATTGTAATACGACTCACTATAGGG ACIAC-IGAIAG(G/A)TGIGAI(G/C)C(G/A)CAIGT

Degeneracy of the probe template was validated by restriction digest with HinfI as previously described (7).

RT-PCR. RNA was isolated from main olfactory epithelia using the PureLink Microto-Midi Total RNA Purification System (Invitrogen). cDNA was reverse-transcribed using the Super-Script III First-Strand Synthesis System (Invitrogen). cDNAs prepared from the various mouse strains were used as PCR templates with Phusion polymerase (Finnzymes) and specific primers pairs designed to amplify <1-kb fragments of *M71*, *MOR28*, *Taar5*, *LacZ*, or *Cre*.

1. Lomvardas S, et al. (2006) Interchromosomal interactions and olfactory receptor choice. *Cell* 126:403–413.
2. Liberles SD, et al. (2009) Formyl peptide receptors are candidate chemosensory receptors in the vomeronasal organ. *Proc Natl Acad Sci USA* 106:9842–9847.
3. Miyamichi K, Serizawa S, Kimura HM, Sakano H (2005) Continuous and overlapping expression domains of odorant receptor genes in the olfactory epithelium determine the dorsal/ventral positioning of glomeruli in the olfactory bulb. *J Neurosci* 25:3586–3592.
4. Magklara A, et al. (2011) An epigenetic signature for monoallelic olfactory receptor expression. *Cell* 145:555–570.
5. Song JS, et al. (2007) Model-based analysis of two-color arrays (MA2C). *Genome Biol* 8:R178.
6. Wen B, Wu H, Shinkai Y, Irizarry RA, Feinberg AP (2009) Large histone H3 lysine 9 dimethylated chromatin blocks distinguish differentiated from embryonic stem cells. *Nat Genet* 41:246–250.
7. Malnic B, Hirono J, Sato T, Buck LB (1999) Combinatorial receptor codes for odors. *Cell* 96:713–723.

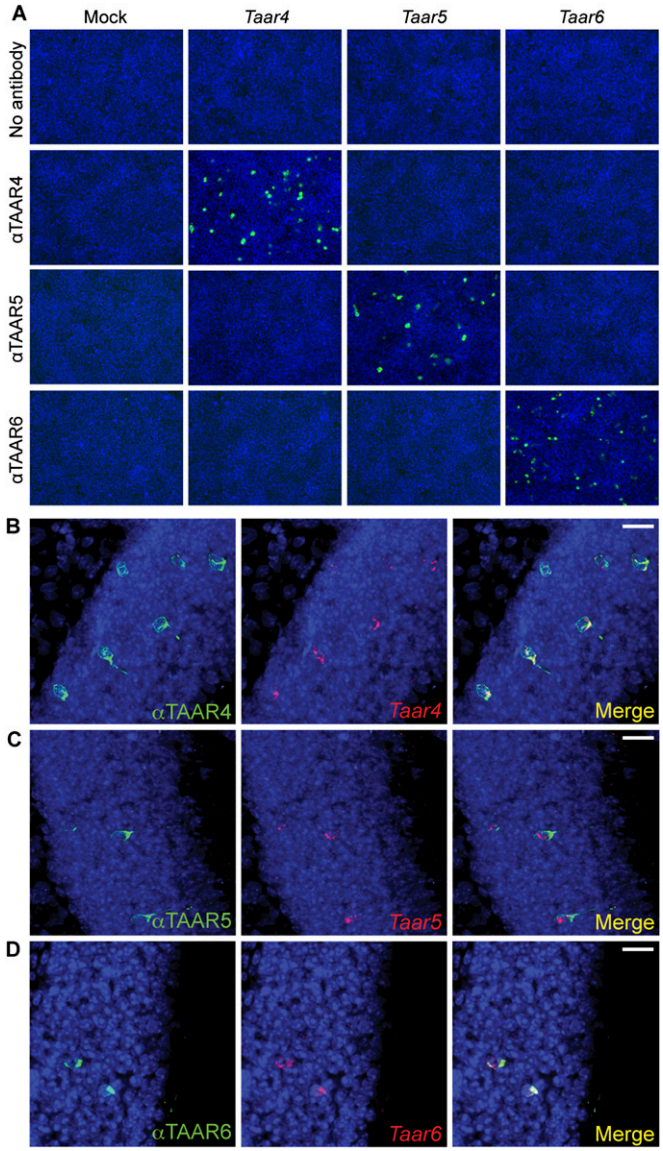

Fig. S1. Validation of the specificity of the antibodies against TAAR4, TAAR5, and TAAR6. (*A*) HEK293 cells were transfected with expression vectors encoding TAAR4, TAAR5, or TAAR6 and stained with the three antibodies. Vertical columns represent HEK293T cells that were transfected either with empty expression vector (Mock) or with an expression vector encoding TAAR4, TAAR5, or TAAR6. Horizontal rows were stained either with no primary antibody or with antibodies specific for TAAR4, TAAR5, or TAAR6. TAAR proteins are stained in green; nuclei are counterstained in blue. (*B–D*) Histological sections through the main olfactory epithelium were analyzed by immunostaining with the antibodies against TAAR4, TAAR5, or TAAR6 (green) and by RNA in situ hybridization with the specific probes for the corresponding receptors (red). Merged images indicate that in all cases identical neurons are detected by both methods. (*B*) TAAR4; (*C*) TAAR5; (*D*) TAAR6. (Scale bars in *B–D*, 20 μm.)

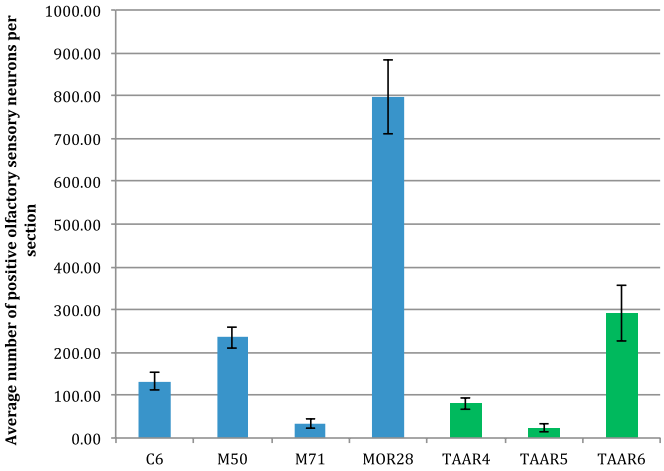

Fig. S2. Expression frequencies of various TAARs and ORs in the main olfactory epithelium. The main olfactory epithelia from three adult C57/Bl6 mice were cryosectioned into 14-μm sections and stained with antibodies against the ORs C6, M50, M71, and MOR28 and the TAARs TAAR4, TAAR5, or TAAR6. The olfactory sensory neurons expressing each of these chemoreceptors were counted in the six consecutive sections with peak expression. The mean and SD of the numbers of positive neurons were calculated from those six sections.

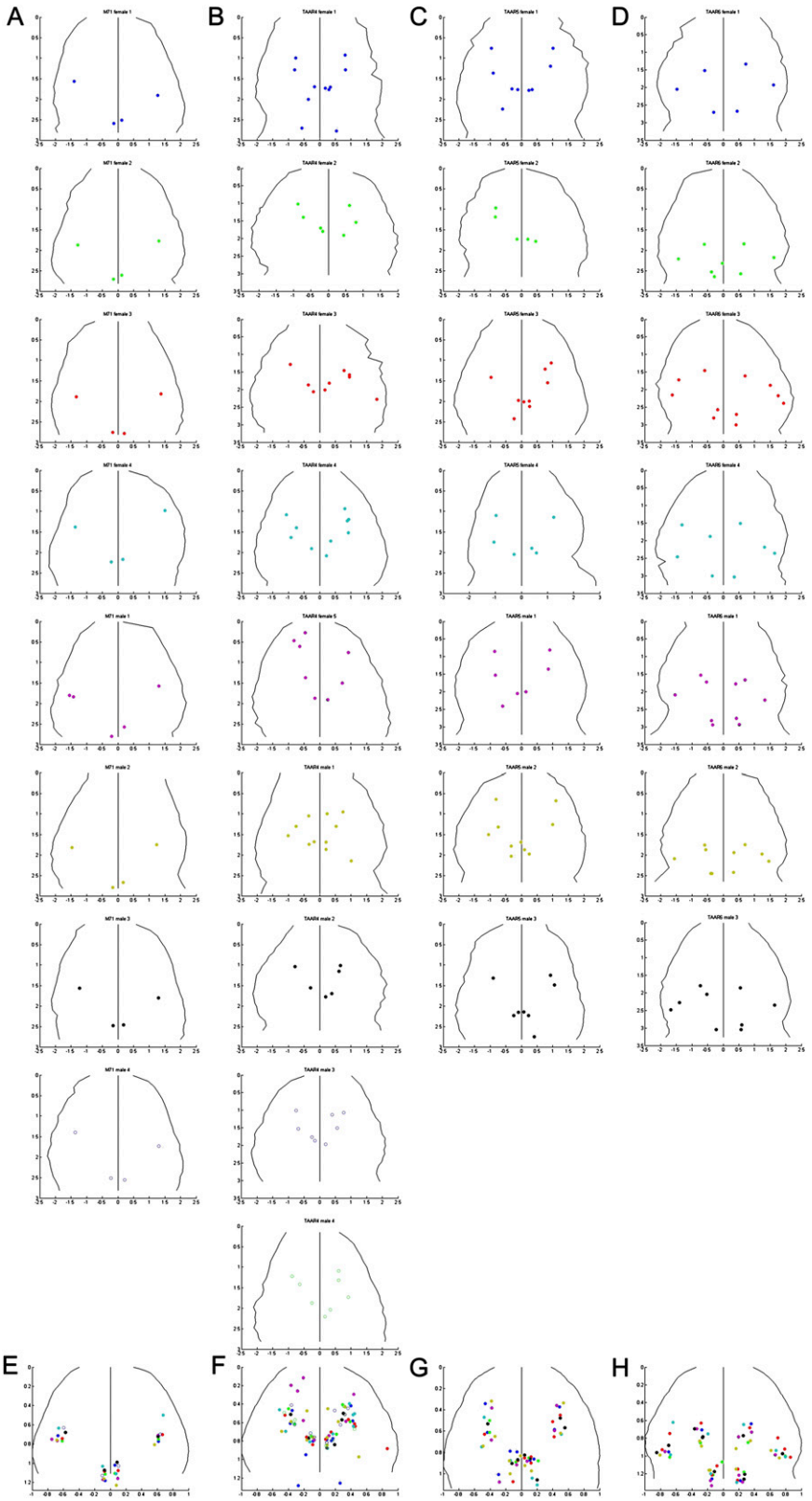

Fig. S3. Distribution of TAAR glomeruli in individual C57/Bl6 mice. (*A* and *E*) M71, (*B* and *F*) TAAR4, (*C* and *G*) TAAR5, (*D* and *H*) TAAR6. Flattened 2D reconstruction of the dorsal aspect of the OB. Top, anterior; bottom, posterior. The distance in mm from the anterior tip of the OB is indicated on the *y* axis. The distance in mm from the midline is indicated on the *x* axis. Maps in *A*–*D* represent individual animals, and maps in *E*–*H* are overlays of glomeruli from all of the individuals plotted for a given TAAR. Mice were 4–6 wk old.

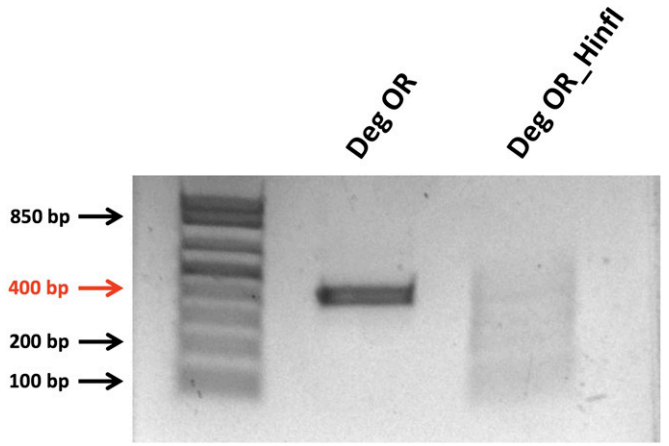

Fig. S4. Validation of the complexity of the degenerate OR probe for in situ hybridization. Degenerate primers were used to amplify OR sequence segments from TM3–TM6. To validate the complexity of the probe, a sample of it was digested with the enzyme HinfI (7). From left to right: lane 1: 1 kb+ DNA ladder; lane 2: undigested template for the degenerate OR probe; lane 3: template for the degenerate OR probe digested with HinfI.

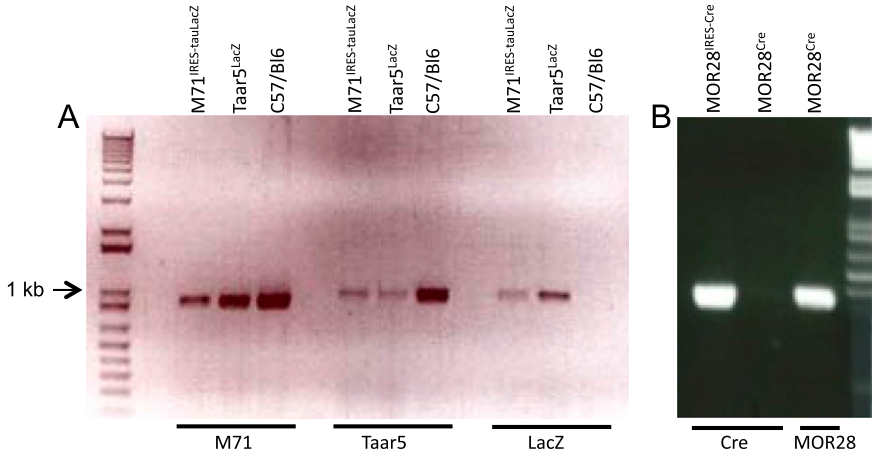

Fig. S5. RT-PCR validation of persistent expression of the *Taar5*^{LacZ} allele. (*A*) PCR amplification of fragments of *M71*, *Taar5*, or *LacZ* using cDNA prepared from main olfactory epithelia from adult *M71*$^{IRES\text{-}tauLacZ}$ mice, in which β-gal is expressed from the genomic locus of the OR *M71* together with the receptor (1); *Taar5*^{LacZ} mice, in which β-gal is expressed from the genomic locus of *Taar5* and replaces the coding sequence of the receptor, or C57/Bl6 mice. (*B*) PCR amplification of fragments of CRE or MOR28 using cDNA prepared from main olfactory epithelia of adult *MOR28*$^{IRES\text{-}CRE}$ or *MOR28*^{CRE} mice in which CRE is expressed from the MOR28 locus either together with the receptor or instead of it, respectively (2). A 1 kb+ DNA ladder was used.

1. Feinstein P, Mombaerts P (2004) A contextual model for axonal sorting into glomeruli in the mouse olfactory system. *Cell* 117:817–831.
2. Shykind BM, et al. (2004) Gene switching and the stability of odorant receptor gene choice. *Cell* 117:801–815.